

LA-UR-01-1668

Approved for public release;
distribution is unlimited.

Title:

**A LARGE AREA DETECTOR BASED COMPUTED
TOMOGRAPHY SYSTEM FOR PRODUCTION
NONDESTRUCTIVE EVALUATION**

Author(s):

Scott Keating and Anthony Davis
Hytec, Inc.
Thomas N. Claytor
Los Alamos National Laboratory

Submitted to:

<http://lib-www.lanl.gov/la-pubs/00818586.pdf>

Los Alamos National Laboratory, an affirmative action/equal opportunity employer, is operated by the University of California for the U.S. Department of Energy under contract W-7405-ENG-36. By acceptance of this article, the publisher recognizes that the U.S. Government retains a nonexclusive, royalty-free license to publish or reproduce the published form of this contribution, or to allow others to do so, for U.S. Government purposes. Los Alamos National Laboratory requests that the publisher identify this article as work performed under the auspices of the U.S. Department of Energy. Los Alamos National Laboratory strongly supports academic freedom and a researcher's right to publish; as an institution, however, the Laboratory does not endorse the viewpoint of a publication or guarantee its technical correctness.

A LARGE AREA DETECTOR BASED COMPUTED TOMOGRAPHY SYSTEM FOR PRODUCTION NONDESTRUCTIVE EVALUATION

LAUR 01 1668

Scott Keating and Anthony Davis

Hytec, Inc.

110 Eastgate Drive

Ph: 505.661.9020

Thomas N. Claytor

Los Alamos National Laboratory

MS C914, 505 667 6216

Los Alamos, NM 87544 U.S.A.

We present a system for industrial x-ray computed tomography that has been optimized for all phases of nondestructive component inspection. Data acquisition is greatly enhanced by the use of high resolution, large area, flat-panel amorphous-silicon detectors. The detectors have proven, over several years, to be a robust alternative to CCD-optics and image intensifier CT systems. In addition to robustness, these detectors provide the advantage of area detection as compared with the single slice geometry of linear array systems.

Parallel processing provides significant speed improvements for data reconstruction, and is implemented for parallel-beam, fan-beam and Feldkamp cone-beam reconstruction algorithms. By clustering ten or more equal-speed computers, reconstruction times are reduced by an order of magnitude. We have also developed interactive software for visualization and interrogation of the full three-dimensional dataset.

Inspection examples presented in this paper include an electro-mechanical device, nonliving biological specimens and a turbo-machinery component. We also present examples of everyday items for the benefit of the layperson.

Keywords: Computed Tomography, X-ray, Cone Beam Tomography

1. INTRODUCTION

Area detector computed tomography systems have been advanced for many years as a possible solution to the problem of industrial inspection. Traditional CT systems are bulky fixed installations tied to a single radiographic source, thus limiting the scope of objects that can be evaluated. Additionally, while traditional linear array systems often excel at producing two-dimensional slices through an object under evaluation, using linear arrays for high-resolution three-dimensional datasets is a very slow process, requiring many hours or days to complete. Recent area detector based CT systems have solved the data acquisition problems, but the computing systems and software have not been up to the task of dealing with the volume of data generated.

In past CT systems, area detectors were employed to acquire three-dimensional datasets more efficiently, but suffered from low resolution, distortion, and alignment difficulties. These problems were addressed by replacing conventional area detectors (e.g., CCD cameras) with large area amorphous silicon (a-Si) flat panel detectors [1-3]. These detectors are capable of returning thousands of lines of data, simultaneously. The advantages of a-Si detectors, however, come with the penalty of having to deal with very large datasets (without magnification, we get approximately 2Mb/cm³ of data). These large datasets present data handling problems for all phases of the data lifecycle, but especially for data processing and visualization. To address these issues, our system hardware and software are designed for accommodation of large datasets.

2. SYSTEM OVERVIEW

The HYTEC CT system consists of four primary elements including the system hardware, data acquisition software, data processing software, and visualization software.

2.1. Hardware and Data Acquisition

Figure 1 shows the current hardware configuration for permanent x-ray source installations. The system includes an a-Si flat panel detector, 3-axis precision staging and a control computer. The control computer is placed outside of the shielded x-ray bay, and communicates with the hardware via a fiber optic line and a single data cable (at distances of over 100 feet). The system hardware is portable and relatively simple to set up, and it can be moved from one source to another in less than an hour.

Data acquisition is performed by the control computer, which is also responsible for staging control and interfacing with the a-Si detector. The data acquisition software allows for remote staging manipulation (for specimen positioning), exposure timing and retrieval of the data from the a-Si detector. This software also performs field flattening and integral-of-attenuation calculations.

The largest a-Si detectors (40 X 30cm) have exposure times on the order of seconds or minutes, depending on test parameters. For smaller specimens, the exposure time may be greatly reduced by use of smaller (25 X 20cm), frame-rate detectors. For these detectors, exposure times can be expected to be on the order of about 1s for typical industrial CT.

Figure 1. CT system (without source) showing large area detector and motion staging.

2.2. Data Processing

Data processing software performs three major functions: sinogram creation, sinogram centering and data reconstruction. Sinograms are created from the corrected image data provided by the data acquisition software. Sinogram centering is necessary to compensate for source-specimen-detector alignment.

As mentioned, datasets returned from the a-Si detectors can be quite large. Parallel-beam and fan-beam reconstructions are typically of order, $O(n^3)$. The Feldkamp cone-beam reconstruction is of order, $O(n^4)$. To reduce the time needed for sinogram creation, centering and reconstruction, we employ a cluster of equal-speed computers (at least 10 CPUs) to perform these calculations. By combining the multi-processor cluster with efficient algorithms, we have reduced the time to reconstruction by at least an order of magnitude.

2.3. Data Visualization

Once the data has been reconstructed, it is necessary to have some meaningful way of visualizing it. To accomplish this task, we use advanced visualization graphics which are capable of resampling and subsampling the data, and of real-time, interactive transformations. Traditional CT visualizations are made by taking “slices” of the volumetric dataset and rendering them as two-dimensional images. The slices are typically orthogonal to the volume coordinates of the dataset. A highly useful feature is to animate the slices in a procession through the volume dataset.

Volume visualizations are also very useful in assessing CT data. By creating real-time volume data transformations, we enable the user to interactively inspect portions of the full three-dimensional dataset from all angles. To enhance volume renderings, voxel (3D pixel) opacity settings are adjusted to allow transmission of data effects through the depth of a volumetric dataset. Additionally, by adding solid or semi-transparent isosurfaces to the volume dataset, features of the data can be highlighted. Most of the features of the data visualization software cannot be reproduced in this static presentation. However, we offer some screen shots of data visualizations produced by this CT system.

3. EXAMPLE DATASETS

We will now look at some of the results generated by the CT system processing and visualization software. In the following sections, we show visualizations of CT datasets for coral, a miniature flashlight, a computer mouse and a cracked plastic specimen.

3.1. Coral

Our first example is a specimen of sea coral. Figure 2 shows a vertical slice through the CT dataset. Figure 3 shows a volume rendering of the coral dataset, including an isosurface.



Figure 1. Photograph of coral.

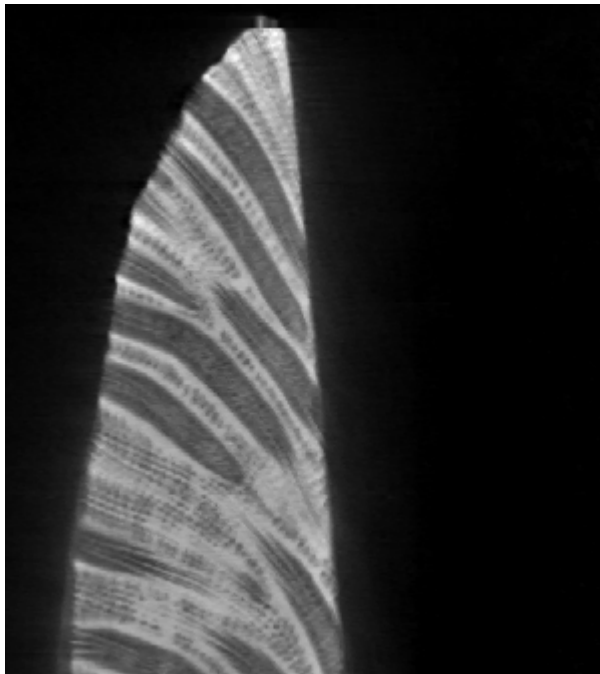


Figure 2. Vertical slice of coral dataset.

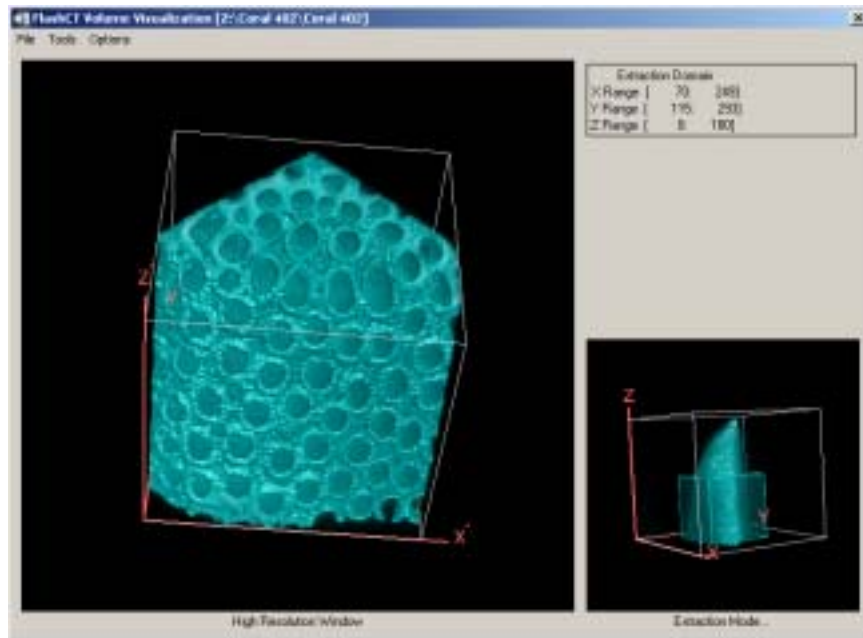


Figure 3. Volume rendering and isosurface of coral dataset.

3.2. Miniature Flashlight

The second dataset example is taken from a miniature key-chain flashlight. Figure 4 shows a photograph of the flashlight alongside a dime to demonstrate scale. Figure 5 shows a vertical slice of the CT dataset. In this image, we can see the flashlight casing, lightbulb(s) and contacts and a cross-section of the AAA-sized battery. Note the cracking of the battery filler material near the tip of the cathode. Figure 6 shows a volume rendering of the subset of the CT data near the spring-battery contact.



Figure 4. Photo of miniature flashlight.

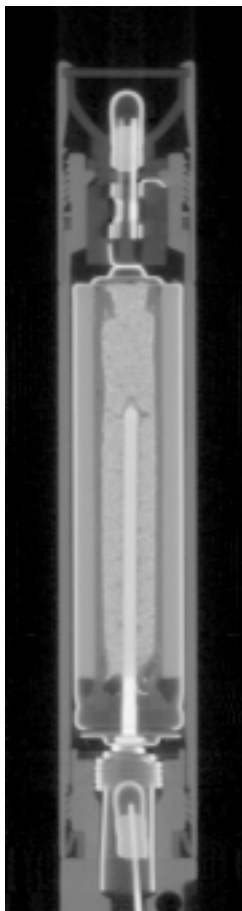


Figure 5. Vertical slice of miniature flashlight dataset.

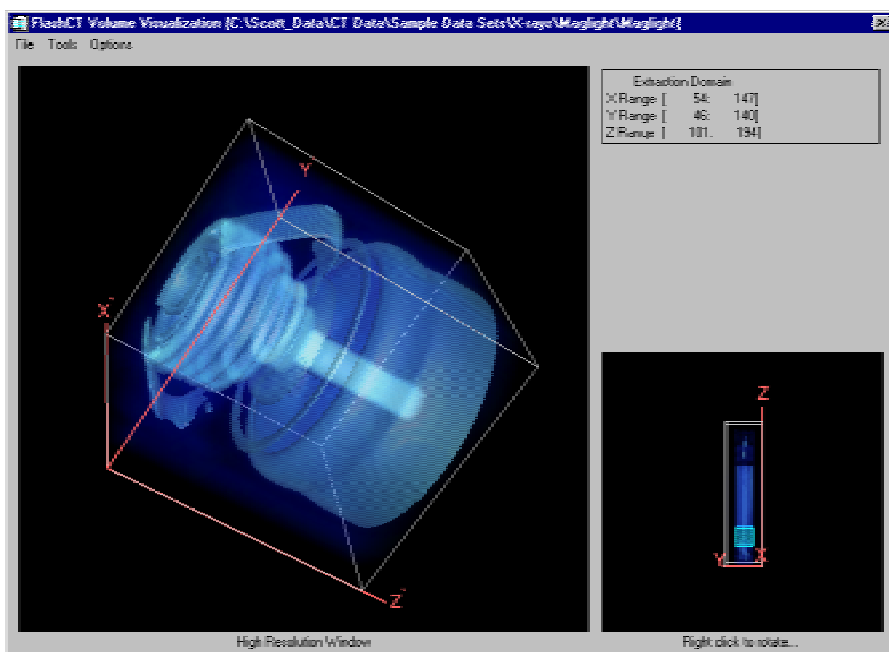


Figure 6. Volume rendering of spring-battery contact zone for miniature flashlight dataset.

3.3. Concrete Core Sample, Neutron CT

The third dataset is for a concrete core sample, and was taken using thermal neutrons at the Los Alamos Neutron Science Center (LANSCE) at Los Alamos National Laboratory. A scintillator sensitive to neutrons was used in a dpiX Flashscan 20 amorphous silicon detector.



Figure 7. Photograph of the concrete sample.

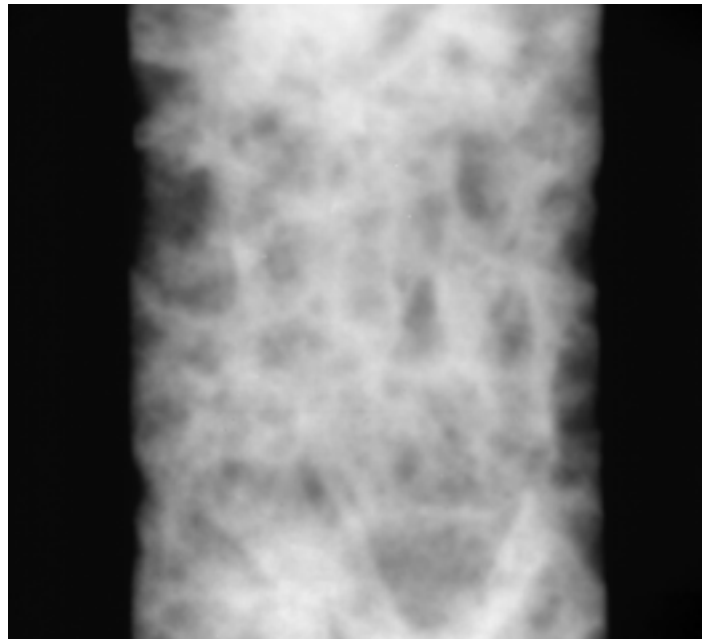


Figure 8. Neutron radiograph of concrete part.

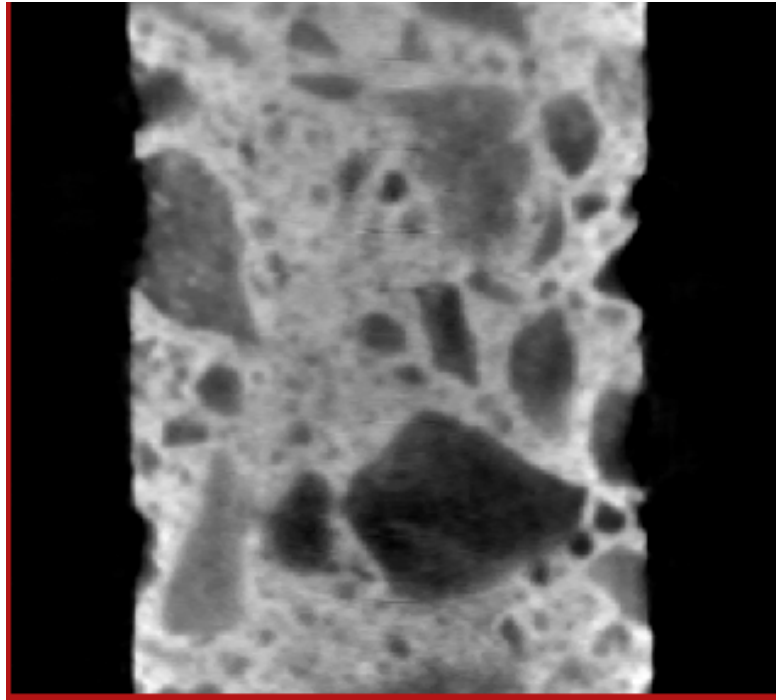


Figure 9. Vertical Slice.

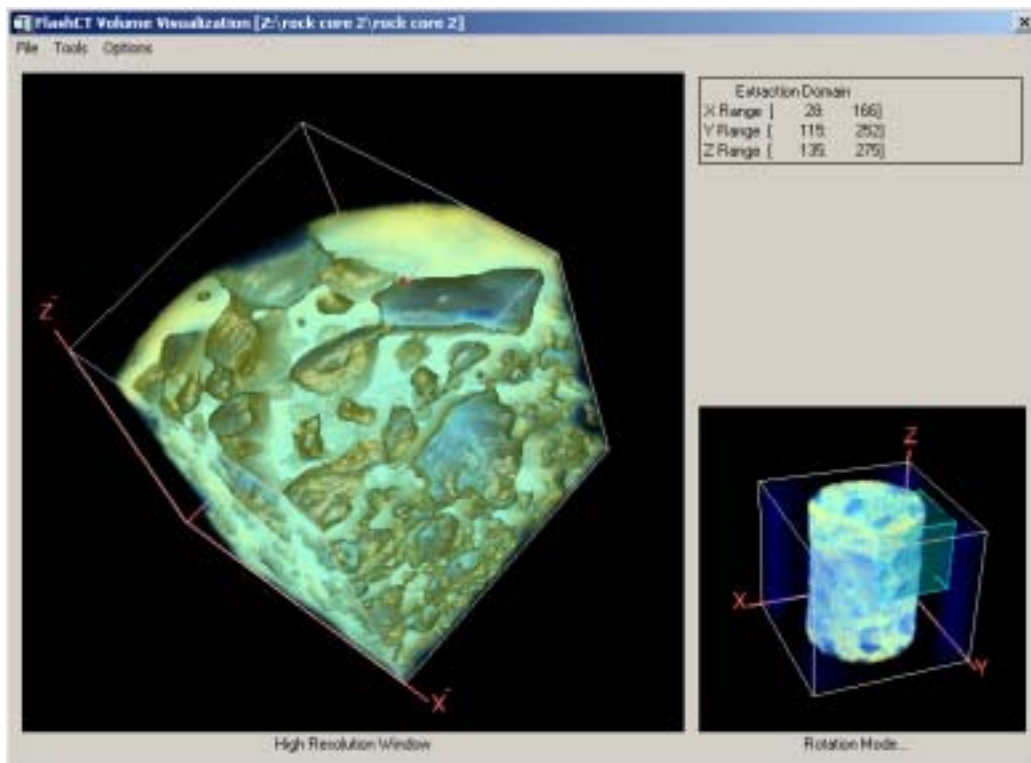


Figure 10. FlashCT VIZ imagery of concrete dataset.

3.4. NASA Two Conductor Connector

Our final dataset is an electrical connector from the NASA space station. The connector was examined for evidence of opens/shorts in the conductors, and the mode of failure.

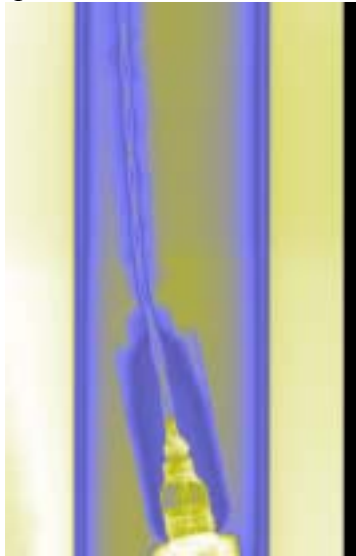


Figure 11. Radiograph of NASA connector.

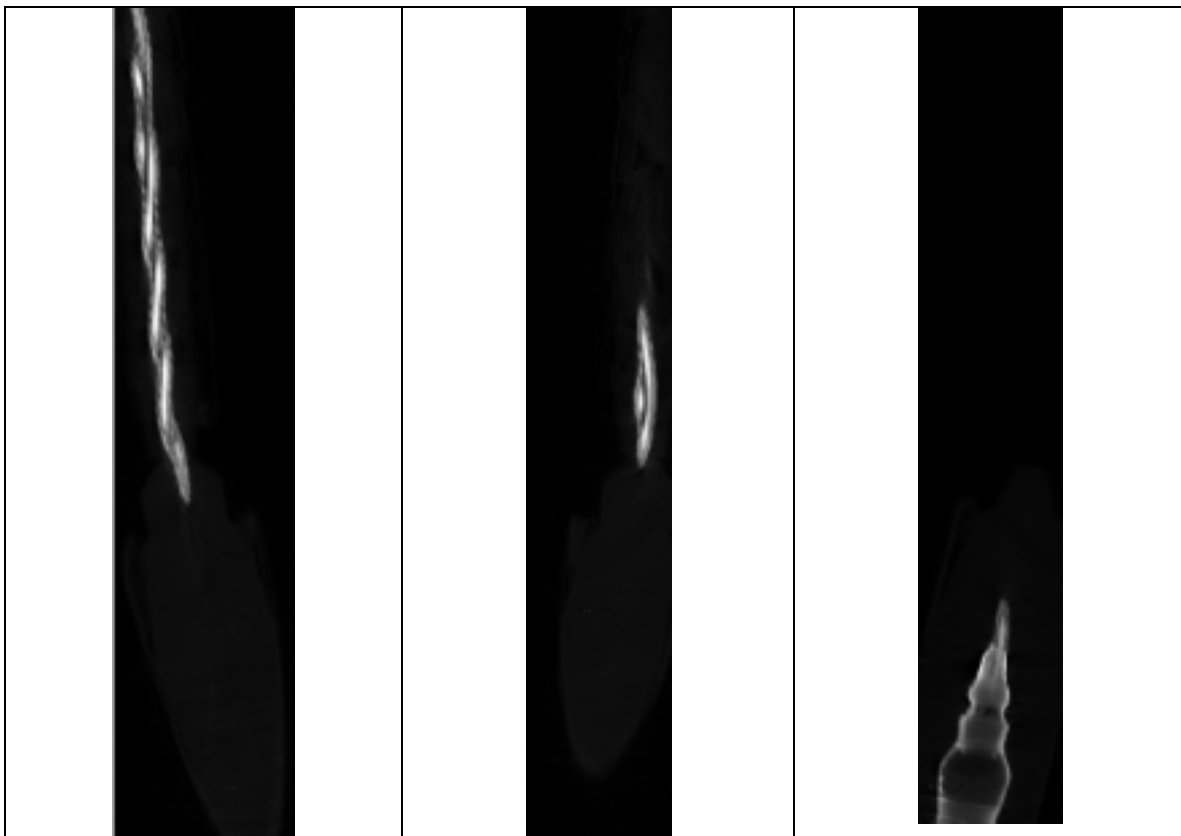


Figure 12. Vertical Slices.

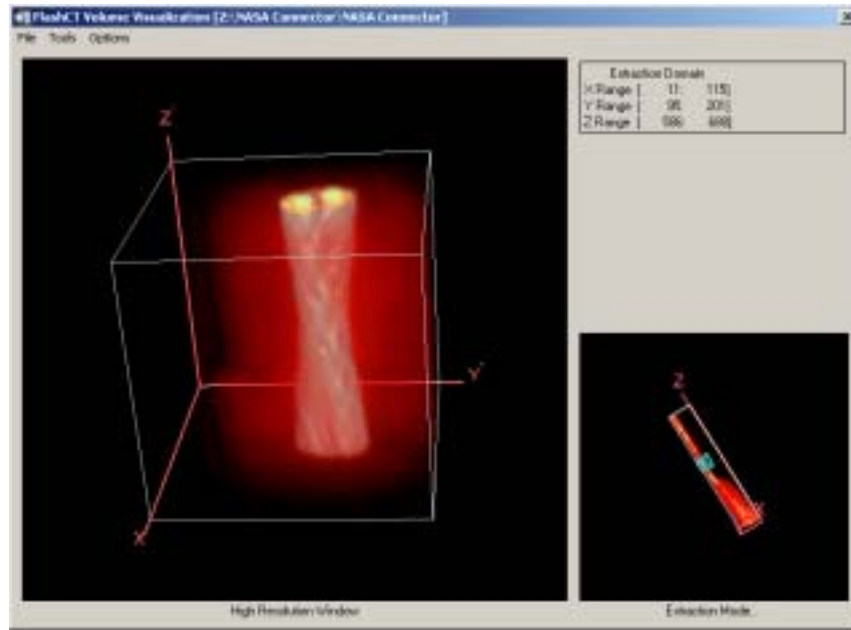


Figure 13. Isosurfaced cladding and rendered wires.

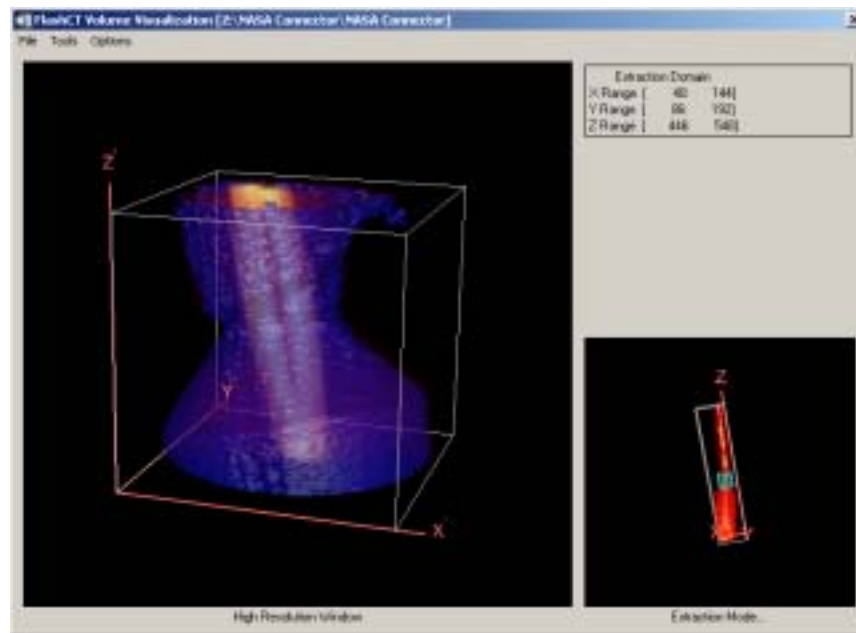


Figure 14. Top of strain relief with isosurfaced outer surface.

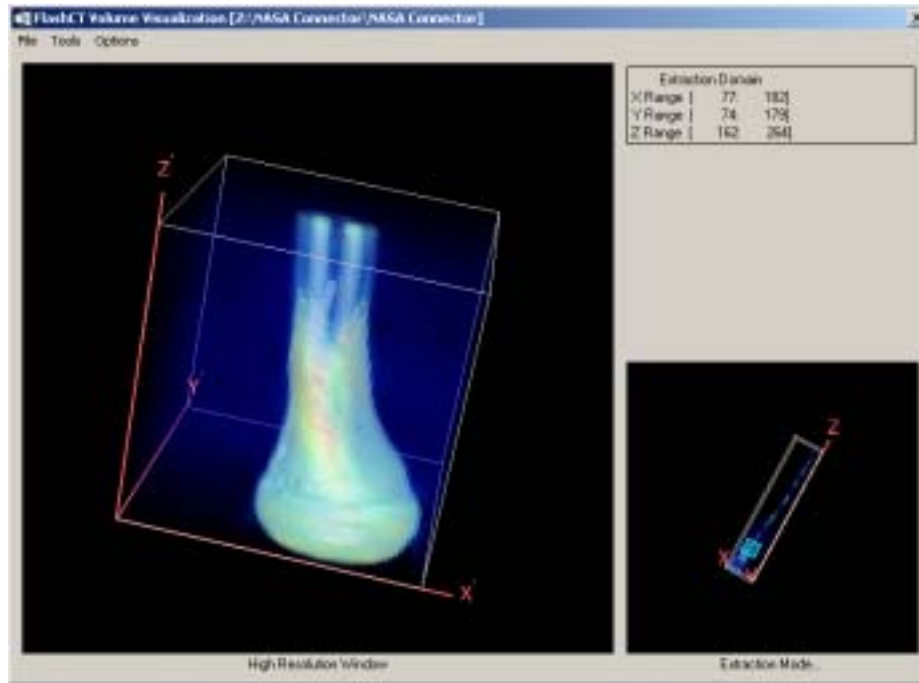


Figure 15. Isosurfaced potting at connector.

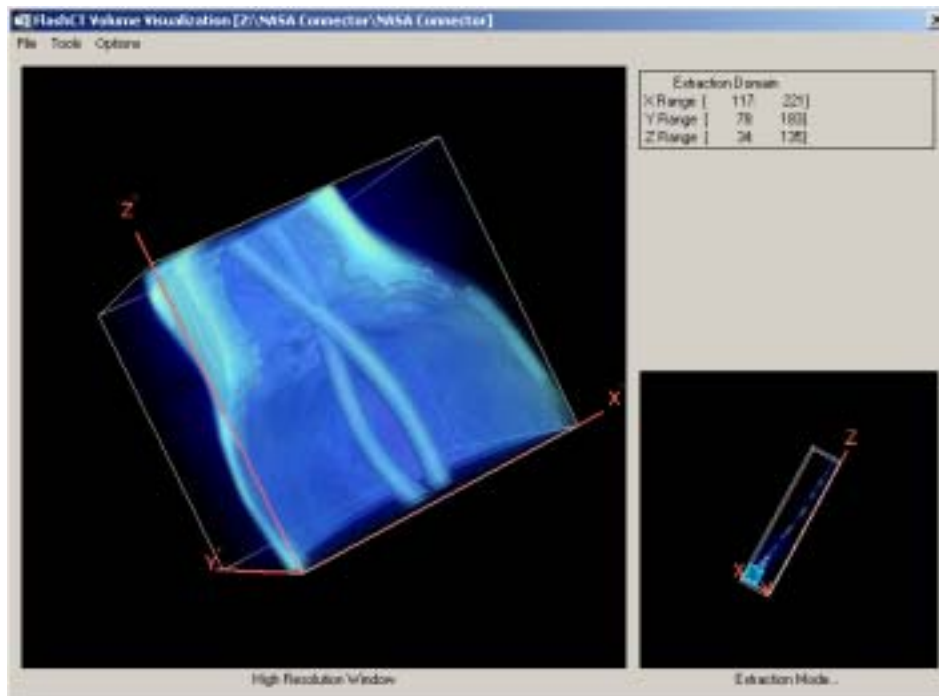


Figure 16. Isosurfaced inner surface of connector, wires.

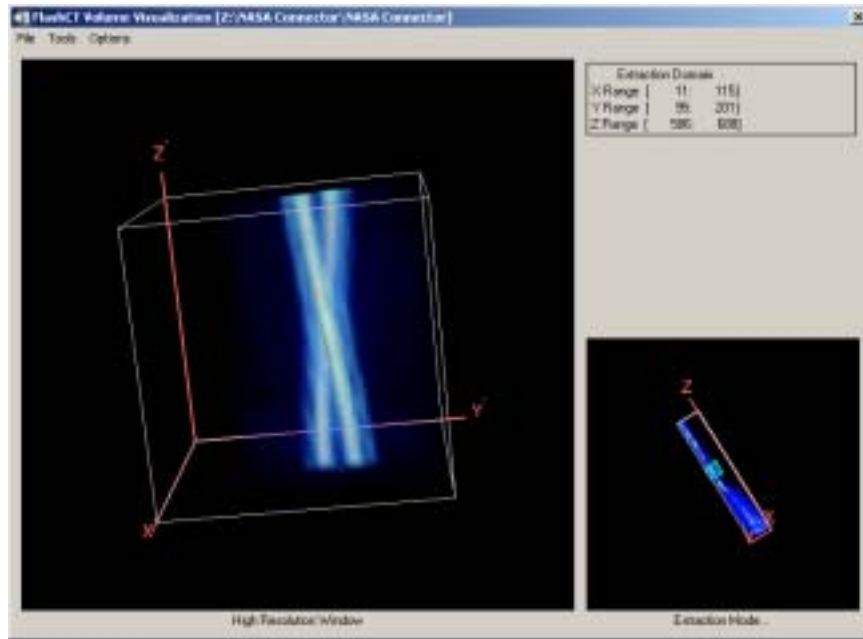


Figure 17. Isosurfaced conductors.

REFERENCES

1. Davis, A. W., Claytor, T. N., Sheats, M. J., 1999, "High-Speed Data Acquisition for Three-Dimensional X-Ray and Neutron Computed Tomography," Proceedings of 1999 SPIE Annual Conference, Denver, CO, LA-UR-99-3136
2. Davis, A. W., Hills, C. R., Sheats, M. J., Claytor, T. N., 2000, "High-energy x-ray and neutron modeling and digital imaging for nondestructive testing applications," Proceedings of 2000 SPIE Annual Conference, San Diego, CA, LA-UR-00-2985.
3. Keating, S. C., 2000, Claytor, T. N., Davis, A. W., and Sheats, M. J., "Technological Advancements for High-Speed Industrial Computed Tomography," Proceedings of 2000 SEI/ASCE Structures Congress, Philadelphia, PA, LA-UR-99-6601.